Published in final edited form as:
Chem Res Toxicol. 2009 May ; 22(5): 863–874. doi:10.1021/tx900042u.

Ascorbic Acid Promotes Detoxification and Elimination of 4-Hydroxy-2(*E*)-nonenal in Human Monocytic THP-1 Cells

Cristobal L. Miranda[†], **Ralph L. Reed**[†], **Heather C. Kuiper**[†], **Susan Alber**[‡], and **Jan F. Stevens**[†,*]

[†]Linus Pauling Institute and the Department of Pharmaceutical Sciences, Oregon State University, Corvallis, OR 97331

[‡]Department of Statistics, Oregon State University, Corvallis, OR 97331

Abstract

4-Hydroxy-2(*E*)-nonenal (HNE), a reactive aldehyde derived from oxidized lipids, has been implicated in the pathogenesis of cardiovascular and neurological diseases, in part by its ability to induce oxidative stress and by protein carbonylation in target cells. The effects of intracellular ascorbic acid (vitamin C) on HNE-induced cytotoxicity and protein carbonylation were investigated in human THP-1 monocytic leukemia cells. HNE treatment of these cells resulted in apoptosis, necrosis and protein carbonylation. Ascorbic acid accumulated in the cells at concentrations of 6.4 mM or 8.9 mM after treatment with 0.1 mM or 1 mM ascorbate in the medium for 18 h. Pretreatment of cells with 1.0 mM ascorbate decreased HNE-induced formation of reactive oxygen species and formation of protein carbonyls. The protective effects of ascorbate were associated with an increase of the formation of GSH-HNE conjugate and its phase-1 metabolites, measured by LC-MS/MS, and with increased transport of GSH conjugates from the cells into the medium. Ascorbate pretreatment enhanced the efflux of the multidrug resistant protein (MRP) substrate, carboxy-2',7'-dichlorofluorescein (CDF), and it prevented the HNE-induced inhibition of CDF export from THP-1 cells, suggesting that the protective effect of ascorbate against HNE cytotoxicity is through modulation of MRP-mediated transport of GSH-HNE conjugate metabolites. Formation of ascorbate adducts of HNE was observed in the cell exposure experiments, but it represented a minor pathway contributing to the elimination of HNE and to the protective effects of ascorbate.

Introduction

Reactive oxygen species (ROS)[1], formed as by-products of cellular redox reactions, are capable of inducing lipid peroxidation of cellular membranes resulting in the formation of α,β-unsaturated aldehydes. The α,β-unsaturated aldehyde, 4-hydroxy-2(*E*)-nonenal (HNE), can be derived from the in vivo oxidation of n-6 fatty acids and is a major product of oxidized low-density lipoprotein. HNE itself can induce oxidative stress in cells by increasing the formation of ROS (1–3). It is well known that low concentrations of oxidants trigger apoptosis while elevated concentrations of oxidants cause necrotic cell death, characterized by disruption of

*To whom correspondence should be addressed. Tel: 541-737-9534. Fax: 541-737-5077. Email: fred.stevens@oregonstate.edu.

[1]Abbreviations: 7-AAD, 7-amino-actinomycin D; AAPH, 2,2'-azobis-2-methylpropanimidamide dihydrochloride; Ac-DEVD-AMC, N-acetyl-Asp-Glu-Val-Asp-AMC (7-amino-4-methylcoumarin); Asc, ascorbic acid; CDF, carboxy-2′,7′-dichlorofluorescein; CDFDA, carboxy-2',7'-dichlorofluorescein diacetate; CM-H_2DCFDA, 5-(and -6)-chloromethyl-2',7'-dichlorodihydrofluorescein diacetate; DCF, dichlorofluorescein; DHN, 1,4-dihydroxy-2(*E*)-nonene; DNPH, 2,4-dinitrophenylhydrazine; DTPA, diethylenetriamine pentaacetic acid; DTT, dithiothreitol; EPI, enhanced product ion; γ-GT, γ-glutamyl transpeptidase; HBSS, Hank's balanced salt solution; HNA, 4-hydroxy-2(*E*)-nonenoic acid; HNAL, HNA lactone; HNE, 4-hydroxy-2(*E*)-nonenal; HRP, horseradish peroxidases; NAcCys, *N*-acetylcysteine; ONA, 4-oxo-2(*E*)-nonenoic acid; ROS, reactive oxygen species; SRM, selected reaction monitoring; SR-VAD-FMK, sulforhodamine-valyl-alanyl-aspartyl-fluoromethyl-ketone.

chromatin distribution and cell membranes. For example, HNE causes necrosis in mouse macrophages at high concentrations (200 μM), but at lower levels of exposure (50–100 μM), HNE produces mostly apoptosis in these cells (4). Most studies on the cytotoxicity of HNE have been focused on apoptosis in various cell types. HNE induces apoptosis in vascular smooth muscle cells (1,5), murine macrophages (4), endothelial cells (6,7), neuronal cells (8, 9), human lens epithelial cells (10), HL-60 cells (11), PC12 cells (2), and 3T3 fibroblasts (12).

In addition to alteration of cellular redox status, HNE may induce cytotoxicity by its ability to react with nucleophilic sites of cellular proteins (13) and DNA (14,15). Oxidative stress and protein carbonylation induced by HNE may contribute to the etiology and/or progression of cardiovascular (e.g., atherosclerosis) and neurodegenerative diseases (e.g., Alzheimer's disease, Parkinson's disease, and cerebral ischemia), cancer and aging. Because of the potential role of HNE-protein adducts in certain human diseases, increased attention has been directed towards finding strategies to inhibit protein carbonylation by lipoxidation-derived reactive carbonyls. One obvious strategy involves the use of free radical scavengers and antioxidants to inhibit the formation of HNE and other lipid peroxidation products. The use of carbonyl-sequestering agents is another promising tool to prevent the formation of HNE-protein adducts (16,17). The generation of drugs sharing both antioxidant and carbonyl scavenger properties represents a new therapeutic opportunity in the treatment of oxidative stress-associated diseases.

Detoxification of HNE is mediated by aldehyde dehydrogenase (ALDH/NAD^+) to form 4-hydroxy-2(*E*)-nonenoic acid (HNA), by aldo-keto reductase (AKR/NADPH) and alcohol dehydrogenase (ADH/NADH) to form 1,4-dihydroxy-2(*E*)-nonene (DHN), and by glutathione *S*-transferases (GSTs) to form the GSH conjugates of HNE and HNA (18–22). GSH-HNE can undergo further metabolism to form GSH-DHN, GSH-HNA, and its lactone form, GSH-HNAL. Many tissues express γ-glutamyl transpeptidase (γ-GT) which catalyzes the conversion of GSH conjugates into the corresponding Gly-Cys conjugates (18). Human monocytes express GSTs (23) and γ-GT (24). The major metabolic conversions of HNE in THP-1 cells are outlined in Scheme 1.

Ascorbic acid (Asc), an antioxidant present in cells at millimolar levels (19), has been shown to protect cells against various types of oxidant injury at physiologically relevant concentrations, e.g., TNFα–induced apoptosis in microvascular endothelial cells (25) and in human umbilical vascular endothelial (HUVEC) cells (26), hypoxia-reoxygenation-induced apoptosis (27), nitrogen dioxide toxicity in HUVEC cells (28), and against β-amyloid-induced cell death and apoptosis in neuroblastoma SH-SY5Y cells (29). Furthermore, Asc exerts a protective effect against oxidized LDL-induced toxicity in THP-1-derived macrophages (30). AAPH-induced oxidative damage in THP-1 cells was likewise decreased by pretreatment of the cells with Asc (31).

In the present study, we investigated the effect of Asc on HNE-induced cytotoxicity, apoptosis, ROS formation, and protein carbonylation, and related these effects to the effects of Asc on the metabolic fate and transport of HNE in human THP-1 monocytes. We selected human monocytic THP-1 cells for our study because ROS-induced monocyte/macrophage interaction with the vascular wall represents an early stage in the pathogenesis of vascular diseases. Monocyte-derived ROS can trigger oxidation of LDL, release of inflammatory cytokines, differentiation of monocytes into (activated) macrophages, and cytokine-induced expression of cell adhesion molecules in nearby vascular endothial cells, all of which are key factors in the development of vascular dysfunction and atherosclerosis (32,33). Understanding the mechanism of the protective effects of Asc at the cellular level may provide a rationale for antioxidant therapy in humans who are at risk for developing cardiovascular disease.

Experimental Procedures

Chemicals

N-acetyl-Asp-Glu-Val-Asp-AMC (7-amino-4-methylcoumarin) (Ac-DEVD-AMC) was purchased from EMD Biosciences, Inc. (San Diego, CA, USA). Fetal bovine serum, phenol red-free RPMI 1640, penicillin, streptomycin, trypsin-EDTA, and chloromethyl-DCF-DA (2′, 7′-dichlorofluorescein diacetate (CM-H_2DCFDA) were procured from Invitrogen (Carlsbad, CA, USA), HNE (for cell exposure experiments) was purchased from Cayman Chemical (Ann Arbor, MI), and MultiCaspase Detection kit was purchased from Guava Technologies (Hayward, CA). Carboxy-2′,7′-dichlorofluorescein (CDF), carboxy-2',7'-dichlorofluorescein diacetate (CDFDA), Sephadex LH-20, ascorbic acid, and sodium ascorbate were from Sigma (St. Louis, MO), and $^{13}C_6$-ascorbic acid was purchased from Omicron Biochemicals (South Bend, IN). For the preparation of GSH, GlyCys and NAcCys adducts, HNE, 4-hydroxy-2(*E*)-nonenoic acid (HNA), and 4-oxo-2(*E*)-nonenoic acid (ONA) were obtained by synthesis during previous work (34).

Cell culture and exposure of THP-1 cells to HNE

THP-1 cells (American Type Culture Collection; Manassas, VA) were routinely cultured in 75 cm^2 flasks in RPMI 1640 medium supplemented with 10% fetal bovine serum (FBS), 2 mM glutamine, 100 units/mL penicillin, 100 μg/mL streptomycin and 0.05 mM 2-mercaptoethanol. The cells were incubated in a humidified atmosphere of 5% carbon dioxide and 95% air at 37 °C.

THP-1 cells were grown in 6-well plates at a density of 3×10^6 cells/mL (2 mL in each well). The cells were pre-incubated with Asc for 18 h in complete culture medium. The cells were washed with PBS or Hank's balanced salt solution (HBSS) to remove Asc and incubated with HNE in HBSS for 3 h. The cells were centrifuged at 1000 g for 5 min to separate the medium (supernatant) from the cells (pellet). The pellet was re-suspended in PBS and lysed by brief sonication on ice unless otherwise stated. Control experiments were conducted in the absence of Asc, HNE, or both. The cells were used for the determination of necrotic cell death, protein carbonyl and ROS formation, caspase-3 and GST activity, and GSH and ATP levels as described below.

Determination of ascorbic acid concentrations in THP-1 cells

Asc was analyzed by ion-pair HPLC with electrochemical detection (35). Briefly, THP-1 cells were incubated with 0, 0.1 or 1.0 mM Asc for 1 or 18 h in phenol red-free RPMI 1640 medium with 10% FBS and 0.05 mM 2-mercaptoethanol. The cells were centrifuged, washed and resuspended in PBS, and counted using a hemacytometer. An aliquot of the cell suspension was mixed with an equal volume of 5% (w/v) metaphosphoric acid containing 1 mM of the metal chelator, diethylenetriamine pentaacetic acid (DTPA), and briefly centrifuged at 10,000 g. Twenty microliters of the supernatant was mixed with 20 μL of 1 mM DTPA/PBS, 12 μL of 2.59 M K_2HPO_4 buffer, pH 9.8, and 148 μL of the HPLC mobile phase (40 mM sodium acetate, 0.54 mM DTPA, 1.5 mM dodecyltriethylammonium phosphate, 7.5% [v/v] MeOH, pH 4.75). A 20 μL aliquot of this mixture was injected onto an LC-8 column (10 cm × 4.6 mm i.d., Supelco, Bellefonte, PA, USA) preceded by a guard column (2 cm × 4.6 mm i.d.) containing the same packing material. The mobile phase was delivered isocratically at a flow rate of 1.0 mL/min. Asc was detected at an applied potential of +600 mV using an LC-4C amperometric electrochemical detector equipped with a glassy carbon working electrode and an Ag/AgCl reference electrode (Bioanalytical Systems, West Lafayette, IN, USA). Before each set of analyses, a calibration was performed using a freshly prepared standard solution of Asc in PBS, containing 1 mM DTPA.

Caspase-3 activity and analysis of apoptotic cells by flow cytometry

Caspase-3 activity of cell lysates was measured by assessing the cleavage of Ac-DEVD-AMC in accordance with the protocol described by Chung et al. (36). Cleavage of the substrate results in the release of AMC which is measured on a fluorescence plate reader (SpectraMax Gemini, Molecular Devices, Sunnyvale, CA) with excitation at 380 nm and emission at 460 nm. The incubation was carried out in 96-well plates in a total volume of 0.2 mL/well. Each well contained 20 μg of protein and 50 μM DEVD-AMC in caspase-3 buffer (25 mM HEPES, pH 7.4, 10% glycerol, and 1 mM EDTA). The increase in fluorescence at various times of incubation at 25 °C was recorded in relative fluorescence units (RFU) following the addition of substrate. The protein content of the cell sample was determined using a Coomassie Plus Protein Assay Kit (Pierce, Rockford, IL, USA) with bovine serum albumin as the standard.

Apoptosis in control and treated THP-1 cells was evaluated by flow cytometry using the MultiCaspase Detection kit according to the manufacturer's directions (Guava Technologies, Hayward, CA). Control and Asc-pretreated cells (1 mM, 18 h) were exposed to HNE (0.1 mM) for 3 h in HBSS and then stained sequentially with SR-VAD-FMK and 7-AAD before analysis by flow cytometry as described by Colgate et al. (37).

Determination of necrotic cell death

THP-1 cells were seeded in 96-well plates and incubated with Asc or PBS (controls) in complete RPMI 1640 medium. Stock solutions of Asc in PBS, buffered to pH 7 with NaOH, were prepared immediately before use. After an 18 h incubation at 37 °C in 5% CO_2, the plates were centrifuged at 200 g and the culture medium was replaced with HBSS, 0.2 mL/well. HNE (in EtOH) was added to each well to a final concentration of 5 to 200 μM. Necrotic cell death was assessed by the trypan blue exclusion method. An equal volume of 0.4% trypan blue was added to a diluted cell suspension. After a 2 min incubation at room temperature, the cells were examined under a light microscope for live and dead cells. Live cells exclude the dye whereas necrotic cells are stained.

Determination of protein carbonyls by ELISA

Protein carbonyls in control and HNE-treated THP-1 cells were analyzed by ELISA (38). Test samples and oxidized BSA standards (Zenith PC Test Kits) were initially reacted with 3 volumes of an aqueous solution containing 10 mM 2,4-dinitrophenylhydrazine (DNPH), 6 M guanidine hydrochloride, and 0.5 M phosphate buffer (pH 2.5), for 45 min at room temperature. Aliquots (200 μL/well, containing 1 μg of protein) of test samples or increasing concentrations of BSA standards were then loaded onto 96-well high-binding ELISA plates. After an overnight incubation at 4 °C, the plates were washed with PBS and then blocked with PBS containing 0.1% Tween 20 (PBS-T) (39). The plates were extensively washed with PBS-T, incubated with 200 μL of biotinylated anti-DNPH rabbit polyclonal antibody per well for 30 min, washed with PBS-T and then incubated with 200 μL of streptavidin-HRP/well for 1 h. The wells were washed before the addition of 200 μL of tetramethylbenzidine-H_2O_2 reagent (Dako, Carpinteria, CA) per well. After a 5 min incubation, 100 μL of 2.5 M sulfuric acid was added to each well to stop the reaction. The absorbance at 450 nm was measured against appropriate blank samples (no DNPH) using a microplate reader (SpectraMax 190).

Determination of intracellular reactive oxygen species (ROS)

The conversion of nonfluorescent CM-H_2DCFDA to fluorescent DCF was used to measure the intracellular production of ROS, mainly, H_2O_2, in THP-1 cells. After exposing Asc-pretreated cells to HNE in 6-well plates for 3 h in HBSS, cells were collected, washed with HBSS, and incubated at a density of 2×10^6/mL with 5 μM CM-H_2DCFDA for 1 h at 37 °C. The cells were centrifuged at 500 g for 5 min and then washed once with HBSS and resuspended

in 200 μL of HBSS. The cells were next transferred to a 96-well plate and the fluorescence intensity was measured with excitation at 485 nm and emission at 530 nm using a fluorescence plate reader (SpectraMax Gemini).

Determination of GSH concentrations in THP-1 cells

GSH concentrations of control and treated THP-1 cells were determined by the method of Hissin and Hilf (40). The reaction mixture (200 μL per well in 96-well plates) consisted of an aliquot of THP-1 cells, 5 mM EDTA, and 0.1 M sodium phosphate buffer, pH 8. The reaction was started by the addition of 10 μL of 1 mg/mL *o*-phthalaldehyde in MeOH. After a 10 min incubation at room temperature, the fluorescence of samples was measured using a flurorescence microplate reader (SpectraMax Gemini) at excitation and emission wavelengths of 350 nm and 420 nm, resp. The GSH concentration of samples was calculated from a standard curve generated by recording the fluorescence of increasing concentrations of GSH loaded on the same 96-well plate used in reading the THP-1 samples.

Glutathione *S*-transferase (GST) activity

GST activity of cell lysates was determined by the method of Habig et al. (41) using 1-chloro-2,4-dinitrobenzene (CDNB) as the substrate. The reaction was carried out in a 96-well plate and the incubation mixture consisted of 50 μg protein, 1 mM GSH, 1 mM CDNB and 0.05 M potassium phosphate in a total volume of 200 μL per well. The reaction was monitored at 340 nm in the kinetic mode using a microplate reader (SpectraMax 190).

Preparation of GSH, CysGly and NAcCys adducts

All adducts were synthesized in the same manner and characterized by LC-ESI-MS/MS. Solutions of GSH, GlyCys or NAcCys (10 mM) were prepared in 0.1 M phosphate buffer, pH 8. To 100 μL-aliquots were added 400 μL of the same phosphate buffer and 400 μL of water. A 1 mM solution of HNE, HNA, or ONA was prepared in EtOH and 100 μL was added to the reaction mixture. The reaction mixtures were stirred at 37 °C for 2 h and acidified to pH 3 with 1 N HCl. The GSH and GlyCys reaction mixtures were loaded onto strata-X SPE columns (60 mg, Phenomenex, Torrance, CA) that were pre-conditioned with 1.2 mL MeCN containing 0.1% HCOOH and equilibrated with 1.2 mL of 0.1% aqueous HCOOH. After sample loading and washing with 0.1% aqueous HCOOH (1.2 mL), the SPE column was eluted with MeCN-0.1% aqueous HCOOH (1:1, v/v) to obtain the GSH and CysGly adducts. The NAcCys adducts were isolated from the corresponding reaction mixtures by solvent extraction with EtOAc (3 × 1 mL) followed by evaporation under nitrogen using a Zymark TurboVap LV (Caliper Life Sciences, Hopkinton, MA), and reconstitution in 1 mL of MeCN:H_2O (20:80, v/v) containing 0.1% HCOOH. 1,4-Dihydroxy-2(*E*)-nonene (DHN) adducts were prepared by reduction of the HNE adducts with 10 μL of a 5 M sodium borohydride solution in 1 N NaOH (42). The reduction mixture was stirred at room temperature for 30 min and then acidified to pH 3 with 1 N HCl. The reduction products were isolated by SPE (GSH-DHN and CysGly-DHN) or extracted with ethyl acetate (NAcCys-DHN), 3 × 1 mL, evaporated under nitrogen, and reconstituted in 1 mL of MeCN:H_2O (20:80, v/v) containing 0.1% HCOOH.

Preparation of ascorbate adducts of HNE (AscHNE)

Sodium ascorbate (1.0 mmol) was dissolved in 10 mL of Milli-Q H_2O. To this solution was added 40 mL of MeCN and 0.5 mL of a solution of HNE (0.1 mmol) in EtOH. After stirring for 5 days at 37 °C, the reaction mixture was concentrated in vacuo, extracted with hexane (2 × 10 mL, discarded) and with EtOAc (3 × 10 mL). The combined EtOAc layers were dried with anhydrous Na_2SO_4 and then the solvent was removed by rotary evaporation. The residue containing crude AscHNE was dissolved in 5 mL of MeOH and chromatographed on a 50 cm × 2.5 cm column filled with Sephadex LH-20 using MeOH as the mobile phase at a flow rate

of 1 mL/min. Fractions (10 mL) were analyzed by loop injection ESI-MS. Fractions containing AscHNE were combined and evaporated under a stream of N_2 gas until constant weight. The residue was dissolved in MilliQ H_2O to yield a 20 mM solution of AscHNE. Alternatively, 200 μL of a 1.0 mM solution of HNE in MeOH and 800 μL of a 6.25 mM solution of ascorbic acid (or $^{13}C_6$-ascorbic acid) were mixed, stirred for 3 h at 37 °C, and directly analyzed by LC-MS/MS.

LC-MS/MS analysis of HNE metabolites in cell media and lysates

Medium samples (400 μL) and lysates (80 μL) were mixed with a two-fold volume of MeCN containing 0.1% HCOOH, centrifuged, and the supernatant analyzed by LC-MS/MS. The data were corrected for the difference in sample volumes. Chromatographic separations were achieved on a 150 mm × 2.1 mm i.d., 4 μm, HydroRP C18 column equipped with a 4.0 × 2.0 i.d. HydroRP guard column (Phenomenex, Torrance, CA). The HPLC solvents were 0.01% aqueous HCOOH (solvent A) and MeCN (solvent B). A linear solvent gradient was used starting from 5% solvent B in solvent A to 100% B over 15 min, followed by elution with 100% B for 5 min at a flow rate of 0.2 mL/min. After returning to the starting conditions in 1 min, the column was equilibrated for 10 min before the next injection. The HPLC system consisted of two Shimadzu Prominence LC-20AD pumps, a Shimadzu SIL-HTC autoinjector and system controller, and a switching valve (Shimadzu, Kyoto, Japan). The column effluent was directed to the mass spectrometer between 2 and 20 min of the chromatographic run and to a waste container during the remainder of the LC run.

The LC-MS/MS instrument consisted of a 4000 QTrap hybrid linear ion trap/triple quadrupole mass spectrometer equipped with a pneumatically-assisted electrospray (Turbo V) source operated at 400 °C (Applied Biosystems/MDS Sciex, Concord, Ontario, Canada). Liquid nitrogen was used as the source of heating/nebulizing, curtain and collision gas. The spray needle was kept at at −4.5 kV in the negative mode. Q1 mass spectra were recorded by scanning in the range 200–1000 at a cycle time of 2 s with a step size of 0.2 u. MS/MS experiments (product ion and precursor ion scanning) were conducted at unit resolution for both Q1 and Q3 with the collision gas set at 'medium'. Enhanced product ion (EPI) scanning was performed by trapping fragment ions (produced in Q2 by collision-induced dissociation) in Q3 (linear ion trap mode) with a dynamic fill time, followed by scanning of Q3 (quadrupole mass analyzer mode). The collision energy was 25 eV in the negative mode, with a collision energy spread of 10 eV. EPI spectra recorded in this manner show fragment ions (trapped in Q3 before scanning) arising from collisions at 15, 25, and 35 eV in the negative ion mode.

The HNE, HNA and DHN adduct preparations were analyzed by LC-MS using Q1 scanning and (enhanced) product ion scanning to determine chromatographic retention times and selected reaction monitoring (SRM) transitions of the molecular ions into fragment ions. The HNA adduct preparations were found to contain HNA lactones (HNAL adducts) in addition to HNA adducts. The following LC-MS/MS characteristics were used for analysis of cell media and lysates (first SRM transition was used for relative quantification, subsequent SRMs used for identity confirmation: GSH-HNE (t_R 10.2 min, *m/z* 462→306, 462→272, 462→254), GSH-DHN (t_R 10.1 min, *m/z* 464→272), GSH-HNA (multiple peaks with t_R 9.8–10.6 min, *m/z* 478→306, 478→272), GSH-HNAL (t_R 11.2 min, *m/z* 460→306, 460→272, 460→254), GlyCys-HNE (multiple peaks with t_R 9–11.5 min, *m/z* 333→177); GlyCys-DHN (multiple peaks with t_R 9–10.3 min, *m/z* 335→143), GlyCys-HNAL (Rt 10.9 min, *m/z* 331→177, 331→143), NAcCys-HNE (t_R 12.0 and 12.2 min, *m/z* 318→189), NAcCys-DHN (t_R 11.6, *m/z* 320→191), NAcCys-HNA (t_R 11.0 min, *m/z* 334→162), NAcCys-HNAL (t_R 13.7 min, *m/z* 316→162, 316→143), α-AscHNE (multiple peaks with t_R 12.4–13.3 min, *m/z* 331→175), and β-AscHNE (multiple peaks with t_R 12.3–13.8 min, *m/z* 331→213). For LC-MS/MS measurement of the GSH and GlyCys adducts of ONA, the SRM transitions *m/z* 476→306 and

476→272 were used for detection of GSH-ONA (t_R 7.8 and 8.0 min), and the SRM transitions *m/z* 347→177, 347→169 and 347→143 for GlyCys-ONA (t_R 6.7 and 6.9 min) using a chromatographic system described by Kuiper *et al*. (34).

CDF retention and efflux studies

THP-1 cells were first incubated with 1 mM Asc or PBS for 18 h, washed with HBSS and then incubated for 3 h in HBSS with 3 μM CDFDA. After 30 min, the cells were washed and re-incubated in CDFDA-free HBSS containing EtOH (vehicle control) or 0.1 mM HNE for 1 or 3 h. Intracellular CDF and CDF released into the medium (efflux) were determined at t = 0 (before incubation) and at 1 and 3 h of incubation with HNE by spectrofluorometry (43).

Determination of intracellular ATP by HPLC

Control and treated THP-1 cells were lysed by vortexing in ice-cold 0.42 M $HClO_4$ solution and then stored at −20 °C for 30 min. The cell lysates were then centrifuged at 14,000 g for 10 min and an aliquot of the supernatant was neutralized with an equal volume of 1 M K_2HPO_4 and re-centrifuged at 14,000 g for 10 min. ATP was measured in cell lysates by ion-pair HPLC with UV detection at 258 nm using a method described by Yeung et al. (44) with modifications. The HPLC equipment consisted of a Waters 600 solvent delivery system, a Waters 717 plus autosampler, a Waters 996 photodiode array detector, a Waters 600 controller and a data acquisition/processing computer with Empower™ software (Waters, Milford, MA). Lysates were separated on a Luna 5 μm C18 column (250 mm × 4.6 mm i.d., Phenomenex, Torrance, CA) using isocratic elution with solvent A (a mixture of 960 mL buffer containing 0.1 M KH_2PO_4 and 0.5 mM tetrabutyl ammonium hydrogen sulfate, 30 mL MeCN, and 10 mL MeOH) and solvent B (MeCN) in the proportion 95:5, v/v, at a flow rate of 0.75 mL/min. ATP eluted at 12.6 min under these conditions and was quantified using a calibration curve constructed from standard solutions containing 0.010, 0.020, 0.050, 0.10, 0.20, 0.50, and 1.00 mg ATP/mL sodium phosphate buffer (0.1 M, pH 7.0).

Statistical analysis

Statistical differences were determined by ANOVA followed by Tukey-Kramer multiple comparison tests. In certain cases, the Student's *t*-test was used to analyze the statistical difference between the control and treatment group. Values of $p < 0.05$ were considered to be statistically significant.

Results

Intracellular Asc in THP-1 cells

First, we investigated whether Asc could be detected in THP-1 cells cultured in phenol red-free RPMI 1640 medium and found that Asc was undetectable in these cells. Then, we examined the effect of adding Asc to the culture medium on the intracellular content of Asc in the cells. Figure 1 shows that intracellular Asc increased about 20 fold by extending the Asc pre-treatment period from 1 h (Panel A) to 18 h (Panel B). At 18 h after incubation with 1 mM Asc, THP-1 cells accumulated Asc to a concentration of 8.9 mM (Figure 1B). After washing the cells with HBSS and incubating for another 3 h in HBSS in the absence of added Asc, the intracellular concentration of Asc was reduced to 4.2 mM (Figure 1C). Incubation of the cells in HBSS with 0.1 mM HNE for 3 h did not significantly change the Asc content of the cells (Figure 1C).

Effects of Asc and HNE on caspase-3 activity

The caspase-3 activity of THP-1 cells was measured to determine if HNE induces apoptosis in these cells through a caspase-dependent pathway. HNE significantly increased caspase-3

activity of THP-1 cells in a dose-dependent manner (Figure 2A). Pretreatment of the cells with 1 mM Asc did not reduce the HNE-induced increase in caspase-3 activity (Figure 2B) or apoptotic cell death (Figure 2C).

Cell death by trypan blue exclusion

Cell death in control and HNE-treated cells was evaluated by the trypan blue exclusion method. Treatment of THP-1 cells with HNE for 3 h in HBSS produced a dose-dependent increase in the number of dead cells (Figure 3A). Pretreatment with 1 mM Asc significantly decreased the number of dead cells in THP-1 cells treated with 0.1 mM HNE (Figure 3B). The 3 h exposure method was chosen because preliminary studies showed that no difference in cell viability measured by trypan blue exclusion was observed between control and HNE-treated cells at 1 h of incubation with lower doses (0.02 to 0.1 mM HNE). Previous studies showed that by using the trypan blue exclusion test, HNE, at low doses (10, 24, or 50 μM) did not cause a reduction in percent cell viability in PC-12 cells in 1 h exposure period but in 2 h exposure or above, these HNE doses were cytotoxic (45).

Protein carbonyls

Exposure of THP-1 cells to 0.1 mM HNE in HBSS for 3 h resulted in a significant increase in the formation of protein carbonyls measured by ELISA using anti-DNP antibodies (Figure 3C). Asc (1 mM) alone did not induce the formation of protein carbonyls. Protein carbonyl formation was significantly decreased when cells were treated with 1 mM Asc for 18 h prior to HNE exposure.

Formation of ROS

Intracellular levels of ROS were measured in control and treated cells using CM-H_2DCFDA which is oxidized to the fluorescent DCF. Exposure to 0.1 mM HNE for 1 or 3 h caused an increase in intracellular ROS as shown by the increase in fluorescence intensity compared to control cells (Figure 4A). ROS production was much greater at 3 h than at 1 h of incubation with 0.1 mM HNE. Pretreatment of the cells with 1 mM Asc significantly reduced the amount of intracellular ROS in THP-1 cells treated with 0.1 mM HNE for 1 or 3 h.

Effects of Asc and HNE on intracellular GSH

The intracellular GSH concentration was not significantly decreased by 1 h exposure to 0.1 mM HNE (Figure 4B). However, after a 3 h incubation with 0.1 mM HNE, a significant reduction in GSH levels in THP-1 cells was observed. Asc pre-treatment prevented the decrease of GSH levels in cells treated with 0.1 mM HNE for 3 h to control levels.

Effects of Asc and HNE on GST activity

The conjugation of HNE with GSH can take place non-enzymatically but enzyme-mediated conjugation by glutathione-*S*-transferases generally predominates (18). Using a global substrate of GST, CDNB, GST activity was significantly decreased when THP-1 cells were treated with 0.1 mM HNE for 3 h (Figure 5) whereas GST activity was not affected by HNE exposure for 1 h (not shown). Asc alone did not alter GST activity but pretreatment with Asc for 18 h prevented the HNE-induced reduction in GST activity of THP-1 cells (Figure 5).

Formation of Asc adducts with HNE

Asc adducts with HNE (AscHNE) were detected in cell media and cell lysates from cells exposed to HNE for 3 h. The AscHNE adducts share the same nominal mass with GlyCys-HNAL, but they are readily distinguished by retention time and by enhanced product ion (EPI) scanning (Figure 6). Two distinct forms of AscHNE were detected, here termed α-AscHNE

and β-AscHNE, which differed from each other with respect to retention times and mass fragmentation (Figure 6). The proportion of α-AscHNE and β-AscHNE found in the medium was 0.96 for both. Although the medium concentrations of Asc were very low after washing the cells and 3 h exposure to HNE, i.e., 1.62 ± 0.2 μM (Asc pre-treatment followed by vehicle exposure) or 2.5 ± 0.2 μM (Asc pre-treatment followed by HNE exposure), it cannot be excluded that the site of Asc formation was in the medium. The total peak area of α-AscHNE and β-AscHNE recorded for the media plus lysates represented 1.2% of the corresponding peak area recorded for GSH-HNE, which is a conservative estimate of amounts because GSH-HNE has an approximately three-fold greater ionization efficiency than β-AscHNE. There was no AscHNE formation in control experiments in which Asc, HNE, or both were left out.

Metabolic fate of HNE in Asc-adequate and Asc-deficient THP-1 cells

Based on our preliminary findings that HNE toxicity in THP-1 cells is more pronounced at 3 h than at 1 h of exposure, we decided to conduct the HNE metabolite studies at 3 h of HNE exposure. HNE metabolites (Scheme 1) in cell media and cell lysates were analyzed by LC-MS/MS and peak areas of six major metabolites were used for statistical analysis (Table 1). The remaining GSH-HNA, GlyCys-HNA and the NAcCys conjugates were detected in small or trace amounts and therefore not further discussed. For GSH-HNE, GSH-DHN, and GSH-HNAL, the proportion $A_{medium}/A_{medium+lysate}$, where A is peak area, ranged from 14 to 30%, whereas these proportions ranged from 61 to 93% for the corresponding GlyCys conjugates.

To examine the effect of Asc on the extent of HNE conjugate formation, the sum of the medium and lysate peak areas, $A_{medium} + A_{lysate}$, for each metabolite was determined for the Asc-adequate and Asc-deficient cells (Table 1). It was found that the Asc-adequate cells produced higher average levels of all six metabolites than the Asc-deficient cells. The increase was only significant for GSH-HNAL ($p = 0.014$). The same increase (16%) was observed for GSH-DHN but it did not reach statistical significance ($p = 0.086$). With regards to the possible effect of Asc on the conversion of GSH conjugates into Gly-Cys conjugates, the Asc-pretreated (Asc-adequate) and control (Asc-deficient) cells showed no difference with respect to the ratio between GlyCys and GSH conjugates found in the medium plus lysate ($p = 0.52$).

The distribution of the six metabolites between medium and cells (lysates) was examined by determining the ratio of peak areas, R, obtained from medium and lysate samples for each metabolite, that is, $R = A_{medium} / A_{lysate}$. The effect of Asc on the distribution of metabolites between medium and cells was estimated by taking the ratio $R_{Asc\text{-}adeq} / R_{Asc\text{-}def}$. These data show that for the metabolites, GSH-HNAL, GSH-DHN, GlyCys-HNE, and GlyCys-DHN, there was a significantly higher proportion of metabolite present in the medium of the Asc-treated cells as compared to the Asc-deficient cells (Table 1, bottom half).

Effect of HNE and Asc on cellular efflux of CDF

CDF is a fluorescent probe for ABC transporters such as ABCC1 (MRP1) and ABCC2 (MRP2) and is generated intracellularly by cleavage of its non-polar, non-fluorescent diacetate form, CDFDA. CDFDA easily diffuses into cells and is cleaved by intracellular esterases to CDF (46). CDF is effluxed from rat hepatocytes via MRP1 (47). Treatment of THP-1 cells with 0.1 mM HNE significantly increased the retention of intracellular CDF as compared to controls at 1 or 3 h of incubation (Figure 7A). In contrast, Asc (1 mM) pretreatment significantly decreased the retention of intracellular CDF in THP-1 cells. Asc pretreatment significantly decreased the HNE-induced retention of CDF in the cells.

CDF released into the medium (extracellular CDF) was also assessed in Asc- and HNE-treated THP-1 cells. As shown in Figure 7B, HNE (0.1 mM) markedly decreased the levels of extracellular CDF after 1 or 3 h of incubation. However, pretreatment of Asc (1 mM) enhanced

the release of CDF into the extracellular medium and partially suppressed the HNE-induced increase in CDF efflux.

Effects of Asc and HNE on intracellular ATP

Pretreatment of THP-1 cells with 1 mM Asc did not significantly alter the levels of ATP but treatment with 0.1 mM HNE caused a marked reduction in ATP levels in these cells (Figure 8). Asc pretreatment partially abolished the HNE-induced reduction of intracellular ATP levels.

Discussion

This study was undertaken to determine the interactions of Asc with the cytotoxic and pro-oxidant lipid peroxidation product, HNE, in a cellular environment. We selected THP-1 cells for our study because ROS-mediated inflammation and activation of monocytes are key factors in the development of vascular dysfunction and atherosclerosis (32) and because THP-1 cells are known to accumulate Asc in millimolar concentrations (31). Our Asc pretreatment protocol produced intracellular Asc levels of 8.9 mM which only dropped to 4.2 mM during our exposure experiments. This is comparable to Asc levels of freshly isolated human monocytes (6 mM) (48). We also determined whether Asc-mediated protection against cytotoxicity was associated with increased metabolic inactivation of HNE. The metabolic fate of HNE has been studied in murine astrocytes (49), human NCTC 2544 keratinocytes (50), and in γ-glutamyl transpeptidase (γ-GT)-overexpressing V79 Chinese hamster lung fibroblasts (51), but these reports do not address the role of Asc in the (metabolic) inactivation of HNE, the focus of our study. We show that pre-incubation of THP-1 cells with Asc exhibited a significant increase in cell viability when exposed to HNE (Figure 3B). The protective effect of Asc against HNE-induced toxicity is analogous to the protection of these cells by 0.8 mM Asc from the cytotoxic effects of AAPH (31).

HNE induces apoptosis in various human cell types but it was not known whether it can also induce apoptosis in THP-1 cells. In THP-1 cells exposed to AAPH, cell death was predominantly due to necrosis rather than by apoptosis based on propidium iodide/Annexin-V staining (52). However, THP-1 cells exhibit classic apoptosis with caspase-3 activation and phosphatidylserine exposure on the plasma membrane upon exposure to oxLDL (53). We found that HNE alone induced apoptosis as assessed by the increase in caspase-3 activity (Figure 2A) and by flow cytometry of cells stained with SR-VAD-FMK, a reagent that binds to activated caspases (Figure 2C). Pretreatment of THP-1 cells with 1 mM ascorbate did not protect cells from apoptosis (Figures 2B and 2C).

HNE-induced ROS formation was more pronounced at 3 h than at 1 h of HNE exposure and was significantly inhibited by pre-incubation of the cells with Asc (Figure 4A). This effect can be explained by the ability of Asc to facilitate metabolic inactivation and cellular excretion, but it is also possible that Asc scavenges ROS (19). In our experiments, THP-1 cells were exposed to HNE in serum-free HBSS that is virtually free of iron and copper, thereby minimizing ROS formation resulting from interaction between Asc and metal ions. Asc can exhibit prooxidant effects on cultured cells when metal ions such as Cu^{2+} are present (54). The increase of ROS levels over time paralleled a greater loss of GSH at 3 h ($p < 0.05$) than at 1 h ($p > 0.05$) compared to the controls (Figure 4B). Pretreatment of THP-1 cells with Asc prevented the HNE-induced decline of cellular GSH levels, which we attribute to scavenging of ROS by Asc and thereby sparing of GSH. Decline of GSH levels by HNE treatment (25–60 μM) was previously observed by Uchida et al. (55) in rat liver epithelial RL34 cells and by Ji et al. (56) in human colorectal carcinoma (RKO) cells. The decline in these studies was maximal at 0.5–2 h and recovered slowly within 4–6 h of HNE exposure. The delayed HNE toxicity (100 μM) and GSH recovery that we observed suggests that THP-1 monocytes are more resistant to oxidative stress than RL34 or RKO cells. Based on our results showing that

0.1 mM HNE exposure for 1 h had no significant effect on apoptotic or necrotic cell death and on GSH (Figure 4B), GST and ATP status, we decided to measure the extent of protein carbonylation and metabolic fate of HNE after 3 h of exposure.

Protein carbonylation represents a plausible explanation for the toxic effects of HNE in THP-1 cells (Figure 3C). HNE can modify proteins through Michael-type addition to cysteine, lysine and histidine residues (13) and through Schiff base formation with lysine (13). Based on the data shown in Figure 3C, it is conceivable that Asc prevents HNE toxicity by preventing or inhibiting the formation of protein-HNE adducts. Asc has been shown to inhibit protein carbonylation produced by irradiation of human plasma by an antioxidant mechanism (57). Some of the proteins adducted by HNE could be crucial for the survival of the THP-1 cells and Asc pretreatment may prevent HNE from damaging these proteins.

It is well-known that Asc can act as a Michael donor to form adducts with α,β-unsaturated aldehydes (58–61), and therefore we hypothesized that Asc competes with GSH for HNE to form AscHNE (Scheme 2). We detected AscHNE in medium and lysate samples of THP-1 cells exposed to HNE (Figure 6), but the levels were very small compared to GSH-HNE and therefore we conclude that Asc conjugation played a minor role in the protection against HNE–induced toxicity. Regarding the formation of AscHNE, we detected two distinct forms, α and β, with different HPLC retention times and different MS/MS spectra (Figure 6). The α-form undergoes retro-Michael fragmentation upon collision-induced dissociation, yielding a prominent Asc fragment ion with *m/z* 175 in the case of AscHNE and with *m/z* 181 in the case of ($^{13}C_6$-Asc)HNE. This suggests that the α-form is the Michael adduct with a single C-C linkage between the Asc and HNE moieties. The β-form does not favor retro-Michael dissociation, but produces an abundant fragment ion with *m/z* 213 in the case of AscHNE and with *m/z* 215 in the case of ($^{13}C_6$-Asc)HNE. This indicates that this fragment ion has retained two carbon atoms from Asc moiety, and we propose that the β-form is analogous with the spiro-form of the Asc adduct of acrolein (58). We observed that the β-form became more abundant over time, suggesting that α-AscHNE is the kinetic product and that β-AscHNE is the thermodynamically favored isomer.

The observation that a much higher proportion of GlyCys conjugates of HNE, DHN and HNAL is found in the medium compared to the corresponding GSH conjugates reflects the extracellular orientation of the active site of γ-GT which converts a wide range of GSH *S*-conjugates into GlyCys *S*-conjugates (62). γ-GT is present in plasma membranes of virtually all cell types including monocytes (24). Because there was no significant difference between Asc-adequate and Asc-deficient cells with respect to the ratio between GlyCys and GSH conjugates ($p = 0.52$), Asc does not appear to have an effect on γ-GT activity in THP-1 cells. Because the GlyCys conjugates are primarily produced from the GSH conjugates outside the cell, we exclude the GlyCys conjugates from further discussion of cellular export of HNE metabolites. The altered medium/lysate ratios listed in the bottom half of Table 1 are therefore likely the result of changes in substrate (HNE metabolite) concentrations in the extracellular medium.

The observation that the presence of millimolar concentrations of Asc inside the cells decreases the formation of HNE adducts of proteins (protein carbonyls) indicates that Asc plays a role in the detoxification of reactive HNE from the cell. The HNE metabolism data summarized in Table 1 show that Asc significantly enhances the formation of the major HNE metabolite, GSH-HNAL, which is likely a reflection of increased cell viability (Figure 3), restoration of GST activity inhibited by HNE (Figure 5), and increased availability of GSH (Figure 4). The effect of Asc on the GSH pool can be attributed to sparing of GSH through scavenging of ROS by Asc (63).

Aldini and co-workers (50) reported the formation of the GSH conjugate of 4-oxo-2(*E*)-nonenal (ONE) from HNE in human NCTC 2544 keratinocytes, suggesting oxidation of the 4-hydroxy group in these cells. We found no evidence for the oxidative conversion of the 4-hydroxyl into the corresponding 4-keto group. The expected major metabolites, i.e., the GSH and GlyCys conjugates of 4-oxo-2(*E*)-nonenoic acid (ONA), were undetectable in our THP-1 media samples by direct LC-MS/MS comparison with synthetic standards.

Active transport of GSH-HNE is mediated by the multidrug resistance-associated protein 2 (MRP2), a member of the ABCC subfamily of ATP-binding cassette (ABC) transporter proteins able to transport organic anions such as GSH conjugates (64,65). MRP2 has been identified as the primary transmembrane protein responsible for export of intracellularly formed GSH-HNE in rat hepatocytes (66) and in Madin-Darby canine kidney II (MDCK II) cells expressing human MRP2 (67). It is also expressed in monocytes (68). In the present study, we utilized the MRP2 substrate, CDF, to examine the hypothesis that one of the protective mechanisms of Asc against HNE-induced cytotoxicity in THP-1 cells is by modulating the function of MRPs. Asc pretreatment was found to enhance the transport of CDF from cells into the surrounding medium as shown by increased levels of extracellular CDF and decreased levels of intracellular CDF (Figure 7). HNE caused a significant reduction in the efflux of CDF whereas Asc pretreatment partially prevented this inhibitory effect of HNE on CDF transport (Figure 7). Our LC-MS/MS measurements of HNE metabolites in media and lysates also demonstrate that Asc promotes the export of two major HNE metabolites, GSH-HNAL and GSH-DHN (Table 1). These findings provide support for our hypothesis that Asc protects against HNE toxicity by facilitating the efflux of GSH conjugates of HNE and its metabolites in THP-1 cells.

Conjugation of GSH with HNE, a reversible reaction, and further phase-1 metabolism and export from cells are all important in preventing HNE from reacting with cellular proteins. One explanation for the Asc-related enhancement of export of GSH conjugates (Table 1) is that Asc promotes the active transport of GSH conjugates from cells into the medium by sparing ATP. HNE induces the formation of ROS (Figure 4A) and ROS is known to decrease intracellular levels of ATP (67), which is consistent with our findings that HNE-induced depletion of ATP is partially restored by Asc (Figure 8). Our results are also consistent with the findings of Hegde and Varma (69), who have shown that Asc restores ROS-induced impaired active transport of Rb^+ in the mouse lens.

Conclusions

We have demonstrated that intracellular Asc reduces the cytotoxic effects of HNE in THP-1 cells using necrotic cell death, protein carbonylation and ROS formation as endpoints. We have also shown that Asc promotes the detoxification and elimination of HNE by enhancing the formation of a major HNE metabolite, GSH-HNAL, and by facilitating cellular export of two major HNE conjugates, GSH-HNAL and GSH-DHN. The Asc-induced increase in medium/lysate ratios of CysGly-HNE and CysGly-DHN was attributed to increased extracellular concentrations of their GSH conjugate precursors (γ-GT substrates) because we found no evidence for an effect of Asc on extracellular activity of γ-GT. We investigated possible mechanisms responsible for the observed effects on metabolite formation and cellular export and found that Asc counteracts the deleterious effects of HNE on GSH and ATP status and that Asc prevents HNE-induced decreases of GST and MRP2 activities. Adducts of Asc with HNE were detected in two isomeric forms, α-AscHNE and β-AscHNE, in media and lysates of washed Asc-adequate cells. AscHNE formation represented a minor pathway in the detoxification and elimination of HNE. Our findings demonstrate that Asc attenuates HNE-mediated oxidative stress in THP-1 cells, which suggests a role for Asc in mitigating inflammatory processes that lead to vascular dysfunction and atherosclerosis.

Acknowledgements

We thank Ms. Deborah J. Hobbs, Linus Pauling Institute, Oregon State University, for the analysis of protein carbonyls and ascorbic acid in THP-1 samples. This study was supported by NIH grants R01HL081721 and S10RR022589. The authors acknowledge the use of the Mass Spectrometry Facility and the Cell Culture Facility of the Environmental Health Sciences Center at Oregon State University (NIH grant P30ES000210).

References

1. Lee JY, Jung GY, Heo HJ, Yun MR, Park JY, Bae SS, Hong KW, Lee WS, Kim CD. 4-Hydroxynonenal induces vascular smooth muscle cell apoptosis through mitochondrial generation of reactive oxygen species. Toxicology Letters 2006;166:212–221. [PubMed: 16919899]
2. Raza H, John A. 4-hydroxynonenal induces mitochondrial oxidative stress, apoptosis and expression of glutathione S-transferase A4-4 and cytochrome P450 2E1 in PC12 cells. Toxicology and Applied Pharmacology 2006;216:309–318. [PubMed: 16843508]
3. Piga R, Saito Y, Yoshida Y, Niki E. Cytotoxic effects of various stressors on PC12 cells: involvement of oxidative stress and effect of antioxidants. Neurotoxicology 2007;28:67–75. [PubMed: 16942797]
4. Li L, Hamilton RF Jr, Kirichenko A, Holian A. 4-Hydroxynonenal-induced cell death in murine alveolar macrophages. Toxicology and Applied Pharmacology 1996;139:135–143. [PubMed: 8685896]
5. Ruef J, Moser M, Bode C, Kubler W, Runge MS. 4-hydroxynonenal induces apoptosis, NF-kappaB-activation and formation of 8-isoprostane in vascular smooth muscle cells. Basic Research in Cardiology 2001;96:143–150. [PubMed: 11327332]
6. Lee JY, Je JH, Kim DH, Chung SW, Zou Y, Kim ND, Ae Yoo M, Suck Baik H, Yu BP, Chung HY. Induction of endothelial apoptosis by 4-hydroxyhexenal. FEBS 2004;271:1339–1347.
7. Herbst U, Toborek M, Kaiser S, Mattson MP, Hennig B. 4-Hydroxynonenal induces dysfunction and apoptosis of cultured endothelial cells. J. Cell. Phys 1999;181:295–303.
8. Mark RJ, Lovell MA, Markesbery WR, Uchida K, Mattson MP. A role for 4-hydroxynonenal, an aldehydic product of lipid peroxidation, in disruption of ion homeostasis and neuronal death induced by amyloid beta-peptide. J. Neurochem 1997;68:255–264. [PubMed: 8978733]
9. Tamagno E, Robino G, Obbili A, Bardini P, Aragno M, Parola M, Danni O. H2O2 and 4-hydroxynonenal mediate amyloid beta-induced neuronal apoptosis by activating JNKs and p38MAPK. Experimental Neurology 2003;180:144–155. [PubMed: 12684028]
10. Choudhary S, Zhang W, Zhou F, Campbell GA, Chan LL, Thompson EB, Ansari NH. Cellular lipid peroxidation end-products induce apoptosis in human lens epithelial cells. Free Radical Biol. & Med 2002;32:360–369. [PubMed: 11841926]
11. Cheng JZ, Singhal SS, Sharma A, Saini M, Yang Y, Awasthi S, Zimniak P, Awasthi YC. Transfection of mGSTA4 in HL-60 cells protects against 4-hydroxynonenal-induced apoptosis by inhibiting JNK-mediated signaling. Archives Biochem. Biophys 2001;392:197–207.
12. Kutuk O, Basaga H. Apoptosis signalling by 4-hydroxynonenal: a role for JNK-c-Jun/AP-1 pathway. Redox Rep 2007;12:30–34. [PubMed: 17263905]
13. Sayre LM, Lin D, Yuan Q, Zhu X, Tang X. Protein adducts generated from products of lipid oxidation: focus on HNE and one. Drug Metabolism Reviews 2006;38:651–675. [PubMed: 17145694]
14. Blair IA. DNA adducts with lipid peroxidation products. J. Biol. Chem 2008;283:15545–15549. [PubMed: 18285329]
15. Feng Z, Hu W, Amin S, Tang MS. Mutational spectrum and genotoxicity of the major lipid peroxidation product, trans-4-hydroxy-2-nonenal, induced DNA adducts in nucleotide excision repair-proficient and -deficient human cells. Biochemistry 2003;42:7848–7854. [PubMed: 12820894]
16. Aldini G, Dalle-Donne I, Facino RM, Milzani A, Carini M. Intervention strategies to inhibit protein carbonylation by lipoxidation-derived reactive carbonyls. Medicinal Research Reviews 2007;27:817–868. [PubMed: 17044003]
17. Negre-Salvayre A, Coatrieux C, Ingueneau C, Salvayre R. Advanced lipid peroxidation end products in oxidative damage to proteins. Potential role in diseases and therapeutic prospects for the inhibitors. British J. Pharmacol 2008;153:6–20.

18. Blair IA. Endogenous glutathione adducts. Current drug metabolism 2006;7:853–872. [PubMed: 17168687]
19. Halliwell, B.; Gutteridge, JM. Free Radicals in Biology and Medicine. Vol. 3 ed. New York: Oxford University Press; 1999.
20. Hayes JD, Flanagan JU, Jowsey IR. Glutathione transferases. Ann. Rev. Pharmacol. Toxicol 2005;45:51–88. [PubMed: 15822171]
21. Traverso N, Menini S, Odetti P, Pronzato MA, Cottalasso D, Marinari UM. Diabetes impairs the enzymatic disposal of 4-hydroxynonenal in rat liver. Free Rad. Biol. & Med 2002;32:350–359. [PubMed: 11841925]
22. Choudhary S, Srivastava S, Xiao T, Andley UP, Srivastava SK, Ansari NH. Metabolism of lipid derived aldehyde, 4-hydroxynonenal in human lens epithelial cells and rat lens. Investigative Ophthalmology & Visual Science 2003;44:2675–2682. [PubMed: 12766072]
23. Darley-Usmar VM, Severn A, O'Leary VJ, Rogers M. Treatment of macrophages with oxidized low-density lipoprotein increases their intracellular glutathione content. Biochem. J 1991;278(Pt 2):429–434. [PubMed: 1898336]
24. Paolicchi A, Minotti G, Tonarelli P, Tongiani R, De Cesare D, Mezzetti A, Dominici S, Comporti M, Pompella A. Gamma-glutamyl transpeptidase-dependent iron reduction and LDL oxidation--a potential mechanism in atherosclerosis. J Investig. Med 1999;47:151–160.
25. Saeed RW, Peng T, Metz CN. Ascorbic acid blocks the growth inhibitory effect of tumor necrosis factor-alpha on endothelial cells. Experimental Biology and Medicine (Maywood, N.J) 2003;228:855–865.
26. Rossig L, Hoffmann J, Hugel B, Mallat Z, Haase A, Freyssinet JM, Tedgui A, Aicher A, Zeiher AM, Dimmeler S. Vitamin C inhibits endothelial cell apoptosis in congestive heart failure. Circulation 2001;104:2182–2187. [PubMed: 11684628]
27. Dhar-Mascareno M, Carcamo JM, Golde DW. Hypoxia-reoxygenation-induced mitochondrial damage and apoptosis in human endothelial cells are inhibited by vitamin C. Free Rad. Biol. & Med 2005;38:1311–1322. [PubMed: 15855049]
28. Tu B, Wallin A, Moldeus P, Cotgreave I. The cytoprotective roles of ascorbate and glutathione against nitrogen dioxide toxicity in human endothelial cells. Toxicology 1995;98:125–136. [PubMed: 7740541]
29. Huang J, May JM. Ascorbic acid protects SH-SY5Y neuroblastoma cells from apoptosis and death induced by beta-amyloid. Brain Research 2006;1097:52–58. [PubMed: 16725131]
30. Kang YH, Park SH, Lee YJ, Kang JS, Kang IJ, Shin HK, Park JH, Bunger R. Antioxidant alpha-keto-carboxylate pyruvate protects low-density lipoprotein and atherogenic macrophages. Free Radical Research 2002;36:905–914. [PubMed: 12420749]
31. Loke WM, Proudfoot JM, McKinley AJ, Croft KD. Augmentation of monocyte intracellular ascorbate in vitro protects cells from oxidative damage and inflammatory responses. Biochem. Biophys. Res. Comm 2006;345:1039–1043. [PubMed: 16712788]
32. Weber C, Zernecke A, Libby P. The multifaceted contributions of leukocyte subsets to atherosclerosis: lessons from mouse models. Nature Reviews 2008;8:802–815.
33. Diaz MN, Frei B, Vita JA, Keaney JF Jr. Antioxidants and atherosclerotic heart disease. New England J. Medicine 1997;337:408–416.
34. Kuiper HC, Miranda CL, Sowell JD, Stevens JF. Mercapturic acid conjugates of 4-hydroxy-2-nonenal and 4-oxo-2-nonenal metabolites are in vivo markers of oxidative stress. J. Biol. Chem 2008;283:17131–17138. [PubMed: 18442969]
35. Suh J, Zhu BZ, Frei B. Ascorbate does not act as a pro-oxidant towards lipids and proteins in human plasma exposed to redox-active transition metal ions and hydrogen peroxide. Free Rad. Biol. & Med 2003;34:1306–1314. [PubMed: 12726918]
36. Chung WG, Miranda CL, Maier CS. Epigallocatechin gallate (EGCG) potentiates the cytotoxicity of rotenone in neuroblastoma SH-SY5Y cells. Brain Research 2007;1176:133–142. [PubMed: 17900545]
37. Colgate EC, Miranda CL, Stevens JF, Bray TM, Ho E. Xanthohumol, a prenylflavonoid derived from hops induces apoptosis and inhibits NF-kappaB activation in prostate epithelial cells. Cancer Letters 2007;246:201–209. [PubMed: 16563612]

38. Buss IH, Winterbourn CC. Protein carbonyl measurement by ELISA. Methods in Molecular Biology (Clifton, N.J) 2002;186:123–128.
39. Mohammad K, Esen A. A blocking agent and a blocking step are not needed in ELISA, immunostaining dot-blots and western blots. J. Immunological Methods 1989;117:141–145.
40. Hissin PJ, Hilf R. A fluorometric method for determination of oxidized and reduced glutathione in tissues. Anal. Biochem 1976;74:214–226. [PubMed: 962076]
41. Habig WH, Pabst MJ, Jakoby WB. Glutathione S-transferases. The first enzymatic step in mercapturic acid formation. J. Biol. Chem 1974;249:7130–7139. [PubMed: 4436300]
42. Hermanson, GT. Bioconjugate Techniques. San Diego: Academic Press, Inc.; 1996.
43. Payen L, Courtois A, Campion JP, Guillouzo A, Fardel O. Characterization and inhibition by a wide range of xenobiotics of organic anion excretion by primary human hepatocytes. Biochem. Pharmacol 2000;60:1967–1975. [PubMed: 11108814]
44. Yeung P, Ding L, Casley WL. HPLC assay with UV detection for determination of RBC purine nucleotide concentrations and application for biomarker study in vivo. J. Pharmaceutical and Biomedical Analysis 2008;47:377–382.
45. Siddiqui MA, Singh G, Kashyap MP, Khanna VK, Yadav S, Chandra D, Pant AB. Influence of cytotoxic doses of 4-hydroxynonenal on selected neurotransmitter receptors in PC-12 cells. Toxicol In Vitro 2008;22:1681–1688. [PubMed: 18672050]
46. Breeuwer P, Drocourt JL, Bunschoten N, Zwietering MH, Rombouts FM, Abee T. Characterization of uptake and hydrolysis of fluorescein diacetate and carboxyfluorescein diacetate by intracellular esterases in Saccharomyces cerevisiae, which result in accumulation of fluorescent product. Applied and Environmental Microbiology 1995;61:1614–1619. [PubMed: 7747975]
47. Zamek-Gliszczynski MJ, Xiong H, Patel NJ, Turncliff RZ, Pollack GM, Brouwer KL. Pharmacokinetics of 5 (and 6)-carboxy-2',7'-dichlorofluorescein and its diacetate promoiety in the liver. J. Pharmacology and Experimental Therapeutics 2003;304:801–809.
48. Bergsten P, Amitai G, Kehrl J, Dhariwal KR, Klein HG, Levine M. Millimolar concentrations of ascorbic acid in purified human mononuclear leukocytes. Depletion and reaccumulation. J. Biol. Chem 1990;265:2584–2587. [PubMed: 2303417]
49. Kubatova A, Murphy TC, Combs C, Picklo MJ Sr. Astrocytic biotransformation of trans-4-hydroxy-2-nonenal is dose-dependent. Chem. Res. Toxicol 2006;19:844–851. [PubMed: 16780364]
50. Aldini G, Granata P, Orioli M, Santaniello E, Carini M. Detoxification of 4-hydroxynonenal (HNE) in keratinocytes: characterization of conjugated metabolites by liquid chromatography/electrospray ionization tandem mass spectrometry. J. Mass Spectrom 2003;38:1160–1168. [PubMed: 14648823]
51. Enoiu M, Herber R, Wennig R, Marson C, Bodaud H, Leroy P, Mitrea N, Siest G, Wellman M. gamma-Glutamyltranspeptidase-dependent metabolism of 4-hydroxynonenal-glutathione conjugate. Arch. Biochem. Biophys 2002;397:18–27. [PubMed: 11747306]
52. Kappler M, Gerry AB, Brown E, Reid L, Leake DS, Gieseg SP. Aqueous peroxyl radical exposure to THP-1 cells causes glutathione loss followed by protein oxidation and cell death without increased caspase-3 activity. Biochimica et Biophysica Acta 2007;1773:945–953. [PubMed: 17509699]
53. Baird SK, Hampton MB, Gieseg SP. Oxidized LDL triggers phosphatidylserine exposure in human monocyte cell lines by both caspase-dependent and -independent mechanisms. FEBS Letters 2004;578:169–174. [PubMed: 15581636]
54. Sakagami H, Satoh K, Hakeda Y, Kumegawa M. Apoptosis-inducing activity of vitamin C and vitamin K. Cellular and Molecular Biology (Noisy-le-Grand, France) 2000;46:129–143.
55. Uchida K, Shiraishi M, Naito Y, Torii Y, Nakamura Y, Osawa T. Activation of stress signaling pathways by the end product of lipid peroxidation. 4-hydroxy-2-nonenal is a potential inducer of intracellular peroxide production. J. Biol. Chem 1999;274:2234–2242. [PubMed: 9890986]
56. Ji C, Amarnath V, Pietenpol JA, Marnett LJ. 4-hydroxynonenal induces apoptosis via caspase-3 activation and cytochrome c release. Chem. Res. Toxicol 2001;14:1090–1096. [PubMed: 11511183]
57. Zbikowska HM, Nowak P, Wachowicz B. Protein modification caused by a high dose of gamma irradiation in cryo-sterilized plasma: protective effects of ascorbate. Free Radical Biology & Medicine 2006;40:536–542. [PubMed: 16443169]
58. Fodor G, Arnold R, Mohacsi T, Karle I, Flippen-Anderson J. A new role for l-ascorbic acid: Michael donor to alpha,beta-unsaturated carbonyl compounds. Tetrahedron 1983;39:2137–2145.

59. Arnold R, Fodor G, Mathelier H, Mohacsi T, Szent-Gyorgyi A. Recent aspects of the chemistry of vitamin C. NFCR Cancer Research Association Symposia 1983:197–219.
60. Fodor G, Sussangkarn K, Arnold R, Mathelier H, Mohacsi T, Mujumdar R, Butterick J, Veltri RW. From methylglyoxal to new immunopotentiating ascorbic acid derivatives. Acta Biochimica et Biophysica Hungarica 1987;22:165–179. [PubMed: 3118623]
61. Fodor G, Sussangkarn K, Mathelier H, Fang K, Arnold R. Stereospecificity of a new reaction of L-ascorbic acid with cis and trans olefinic 1,4-dicarbonyl compounds. J. Org. Chem 1986;51:3148–3150.
62. Lieberman MW, Barrios R, Carter BZ, Habib GM, Lebovitz RM, Rajagopalan S, Sepulveda AR, Shi ZZ, Wan DF. gamma-Glutamyl transpeptidase. What does the organization and expression of a multipromoter gene tell us about its functions? Am. J Pathol 1995;147:1175–1185. [PubMed: 7485380]
63. May JM. How does ascorbic acid prevent endothelial dysfunction? Free Radical Biology & Medicine 2000;28:1421–1429. [PubMed: 10924860]
64. Zhou SF, Wang LL, Di YM, Xue CC, Duan W, Li CG, Li Y. Substrates and inhibitors of human multidrug resistance associated proteins and the implications in drug development. Current Medicinal Chemistry 2008;15:1981–2039. [PubMed: 18691054]
65. Sultana R, Butterfield DA. Oxidatively modified GST and MRP1 in Alzheimer's disease brain: implications for accumulation of reactive lipid peroxidation products. Neurochemical Research 2004;29:2215–2220. [PubMed: 15672542]
66. Reichard JF, Doorn JA, Simon F, Taylor MS, Petersen DR. Characterization of multidrug resistance-associated protein 2 in the hepatocellular disposition of 4-hydroxynonenal. Arch. Biochem. Biophys 2003;411:243–250. [PubMed: 12623073]
67. Ji B, Ito K, Horie T. Multidrug resistance-associated protein 2 (MRP2) enhances 4-hydroxynonenal-induced toxicity in Madin-Darby canine kidney II cells. Chem. Res. Toxicol 2004;17:158–164. [PubMed: 14967003]
68. Janneh O, Owen A, Chandler B, Hartkoorn RC, Hart CA, Bray PG, Ward SA, Back DJ, Khoo SH. Modulation of the intracellular accumulation of saquinavir in peripheral blood mononuclear cells by inhibitors of MRP1, MRP2, P-gp and BCRP. AIDS (London, England) 2005;19:2097–2102.
69. Hegde KR, Varma SD. Protective effect of ascorbate against oxidative stress in the mouse lens. Biochimica et Biophysica Acta 2004;1670:12–18. [PubMed: 14729137]

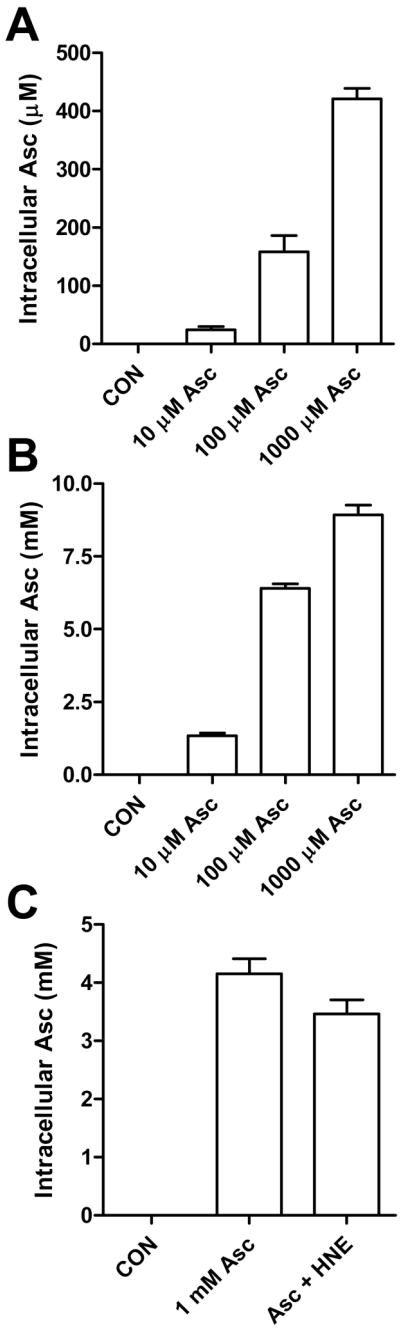

Figure 1.

Intracellular concentration of ascorbic acid (Asc) in THP-1 cells after incubation with Asc (0.01, 0.1 or 1 mM) for 1 h (Panel A) or 18 h (Panel B) in complete RPMI 1640 medium. In Panel C, the cells pre-incubated with 1 mM Asc for 18 h were washed with HBSS and incubated with 100 μM HNE in HBSS for 3 h before Asc analysis. The data are expressed as means ± SE of 3 experiments.

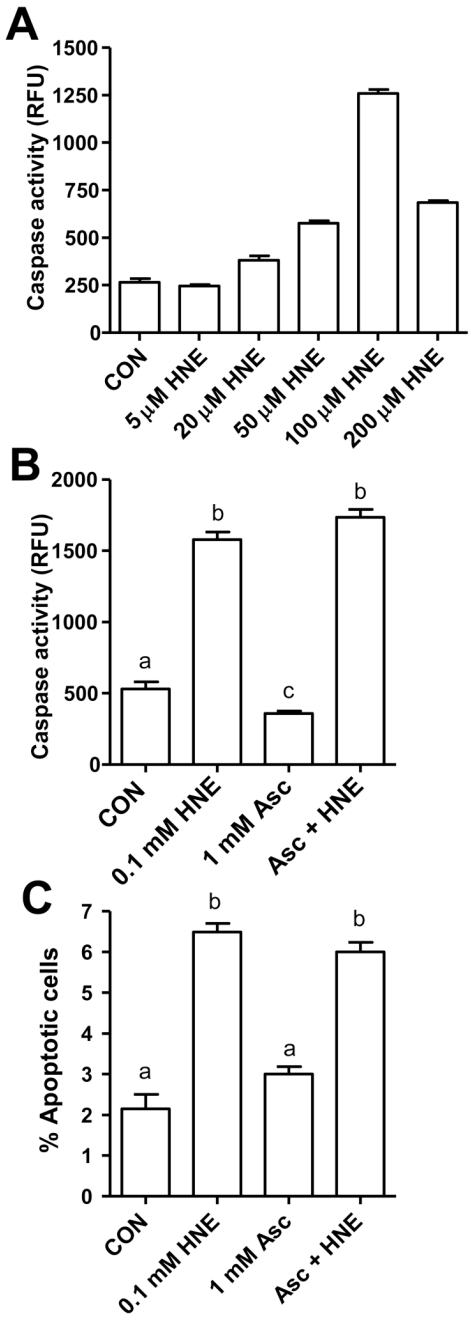

Figure 2.

Effect of HNE exposure (3 h) and Asc on caspase-3 activity of THP-1 cells and on the induction of apoptosis in THP-1 cells. In Panel A, caspase-3 activity of THP-1 cells was determined after treatment of cells with increasing concentrations of HNE. In Panel B, caspase-3 activity was measured in cells exposed to 0.1 mM HNE after pretreatment with 1 mM Asc for 18 h and expressed in relative fluorescence units (RFU). Panel C shows the percentage of apoptotic cells representing the total of early, mid- and late-stage apoptotic cells determined by flow cytometry. The data are expressed as means ± SE of 3 experiments. In Panel A, treatments with HNE ≥ 20 μM were significantly different from the control group (Student's *t*-test, $p < 0.05$). Data in panels B and C were analyzed by one-way analysis of variance (ANOVA)

followed by the Tukey-Kramer multiple comparison post hoc test. Values are statistically different ($p \leq 0.05$) from each other except when sharing a common letter.

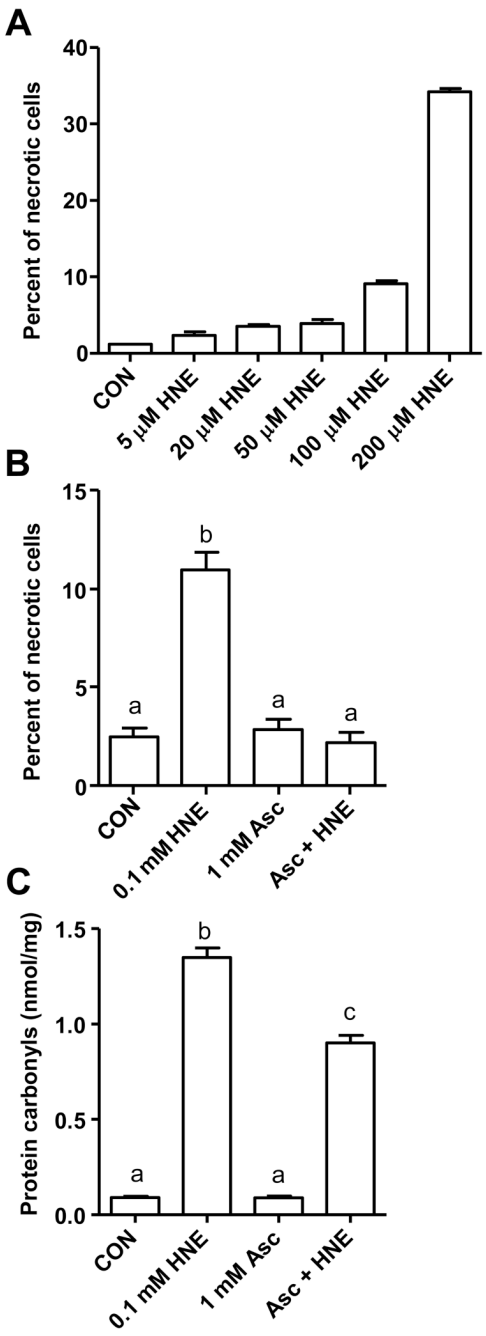

Figure 3.

Effect of Asc on HNE-induced cytotoxicity and on formation of protein carbonyls in THP-1 cells. In Panel A, the cells were exposed to different concentrations of HNE in HBSS for 3 h before staining them with trypan blue. The dead cells (stained with trypan blue) were counted under the microscope and expressed as a percent of total number of cells counted (live + dead). Pretreatment of THP-1 cells for 18 h with 1 mM Asc decreases the extent of necrotic cell death induced by 0.1 mM HNE (panel B) and protein carbonylation (panel C). The data are expressed as means ± S.E. of 3 experiments. In Panel A, treatments with HNE ≥ 20 μM were significantly different from the control group (Student's *t*-test, $p < 0.05$). Data in panels B and C were analyzed by one-way analysis of variance (ANOVA) followed by the Tukey-Kramer multiple

comparison post hoc test. All values are statistically different ($p \leq 0.05$) from each other except when sharing a common letter.

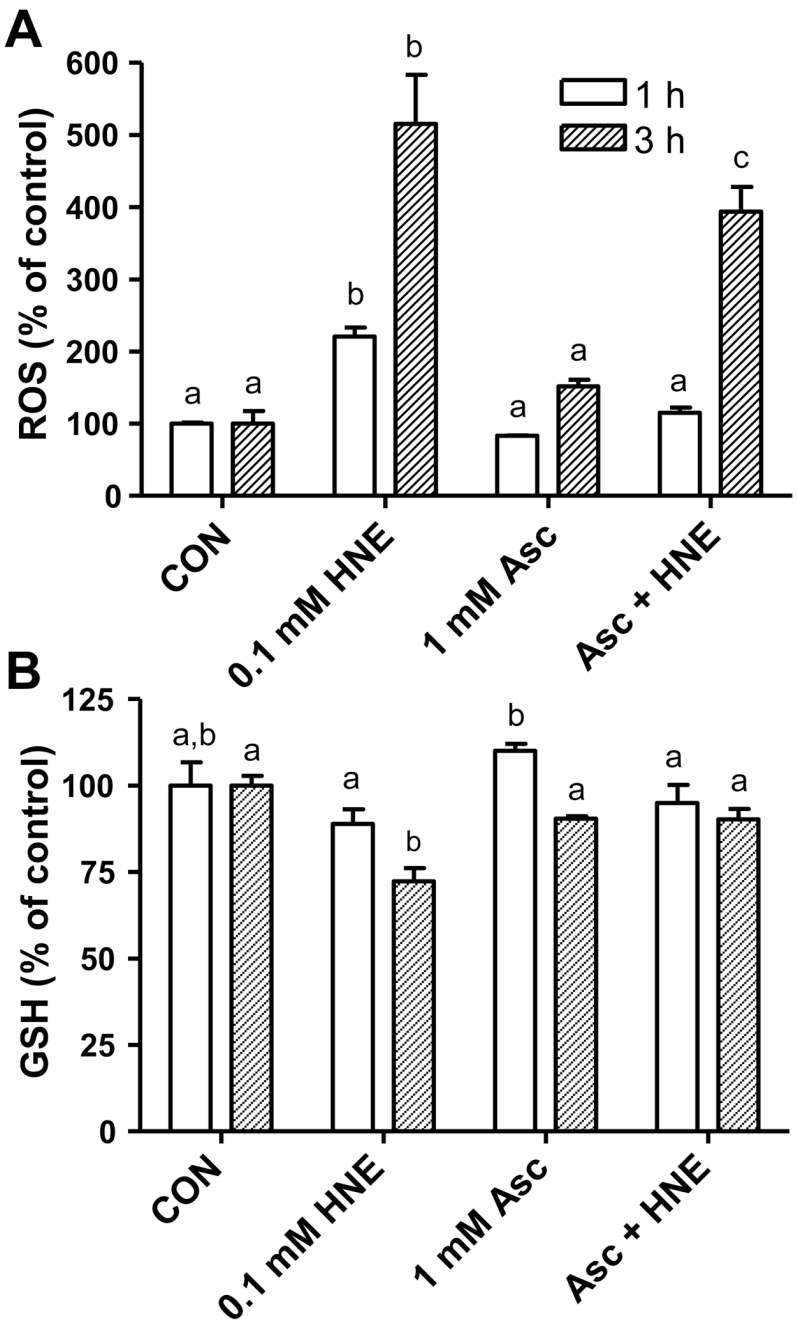

Figure 4.

Effect of Asc on HNE-induced formation of ROS (panel A) and HNE-induced depletion of GSH (panel B). In Panel A, the cells were incubated with Asc (1 mM) for 18 h, washed and reincubated for 1 or 3 h in HBSS with or without HNE (0.1 mM) prior to the addition of 5 μM CM-H_2DCFDA. ROS production was indicated by the increase in fluorescence measured at excitation wavelength of 485 nm and emission wavelength of 530 nm. In Panel B, control and Asc-pretreated THP-1 cells were incubated with 0.1 mM HNE for 1 or 3 h before GSH analysis. The data are expressed as means ± SE of 3 experiments. The GSH content of control cells was 10.2 nmol/mg protein. Data were analyzed by one-way analysis of variance (ANOVA)

followed by the Tukey-Kramer multiple comparison post hoc test. Within the 1 h or 3 h data set, values are statistically different ($p \leq 0.05$) except when sharing a common letter.

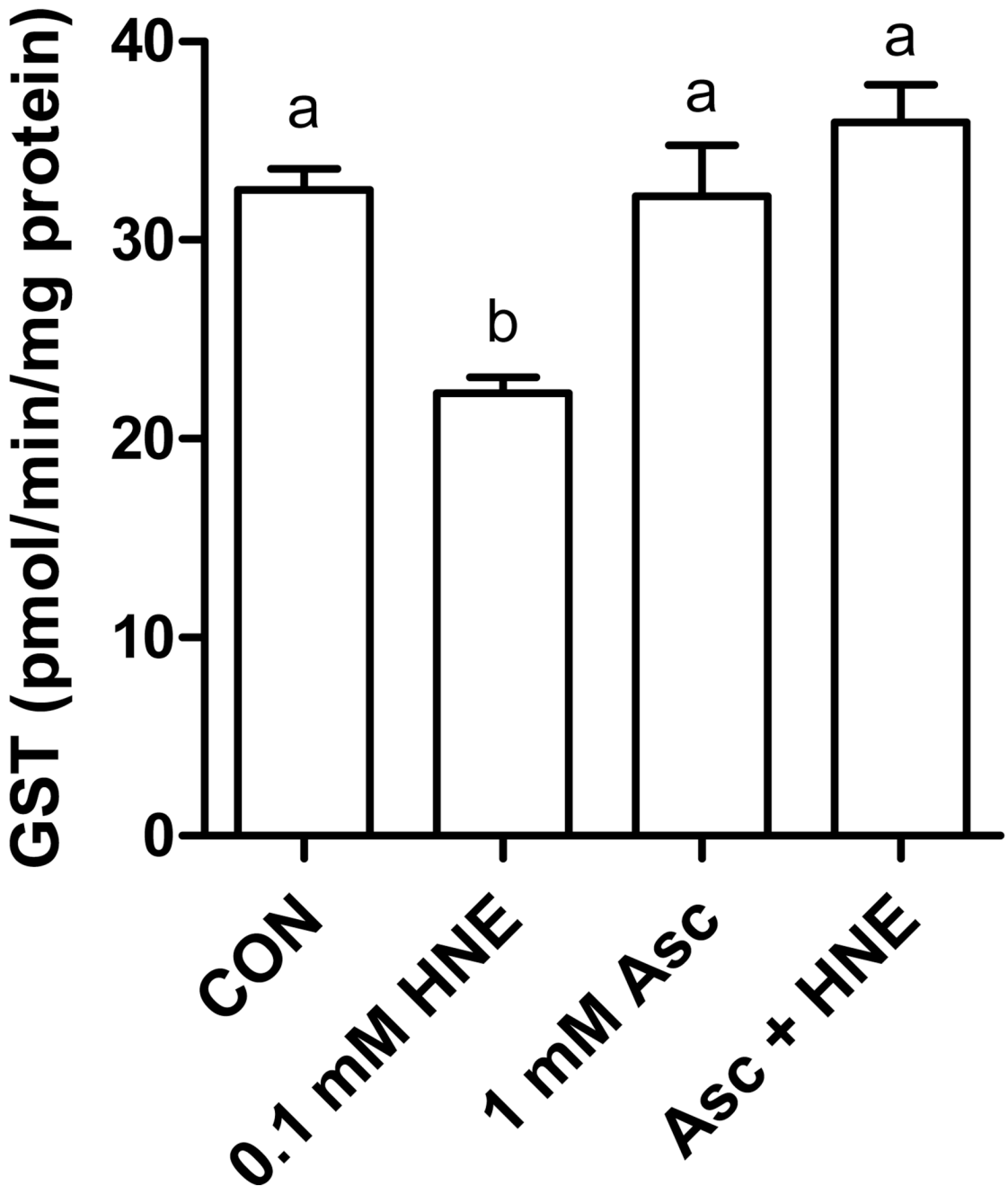

Figure 5.

Effect of Asc and HNE on GST activity of THP-1 cells. The cells were pre-incubated with 1 mM Asc for 18 h, washed with HBSS and then incubated with 0.1 mM HNE in HBSS for 3 h before GST analysis. The data are expressed as means ± SE of 3 experiments. Data were analyzed by one-way analysis of variance (ANOVA) followed by the Tukey-Kramer multiple comparison post hoc test. All values are statistically different ($p \leq 0.05$) from each other except when sharing a common letter.

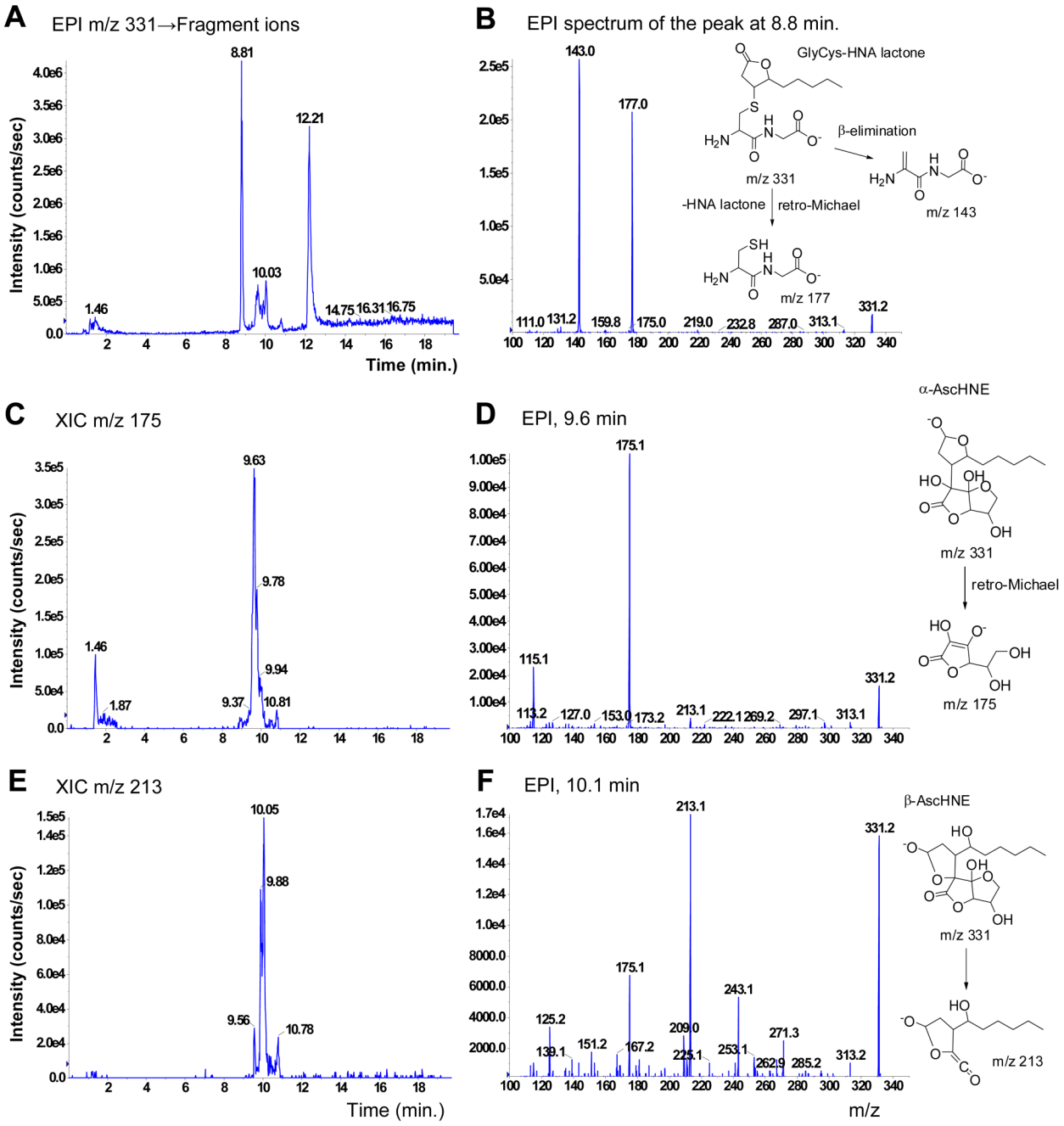

Figure 6.

LC-MS/MS Analysis of the medium of THP-1 cells after treatment with ascorbic acid and HNE. Panel A shows the total ion current chromatogram obtained by enhanced product ion (EPI) scanning of ions with *m/z* 331. The peak at 8.8 min was identified as GlyCys-HNAL (panel B). AscHNE eluted as a multiplet of peaks due to the presence of isomers. The early eluting isomers (9.6 min) yielded ascorbate with *m/z* 175 as the main fragment ion (Panels C and D), while the isomers eluting around 10.1 min (panel E) resisted retro-Michael fragmentation and showed a base peak at *m/z* 213 in the EPI spectrum (panel F). The peak at 12.2 min in panel A was present in all media and control samples, and it was therefore not

further investigated. The longer retention times listed under ‘LC-MS/MS analysis of HNE metabolites’ are due to the use of a guard column.

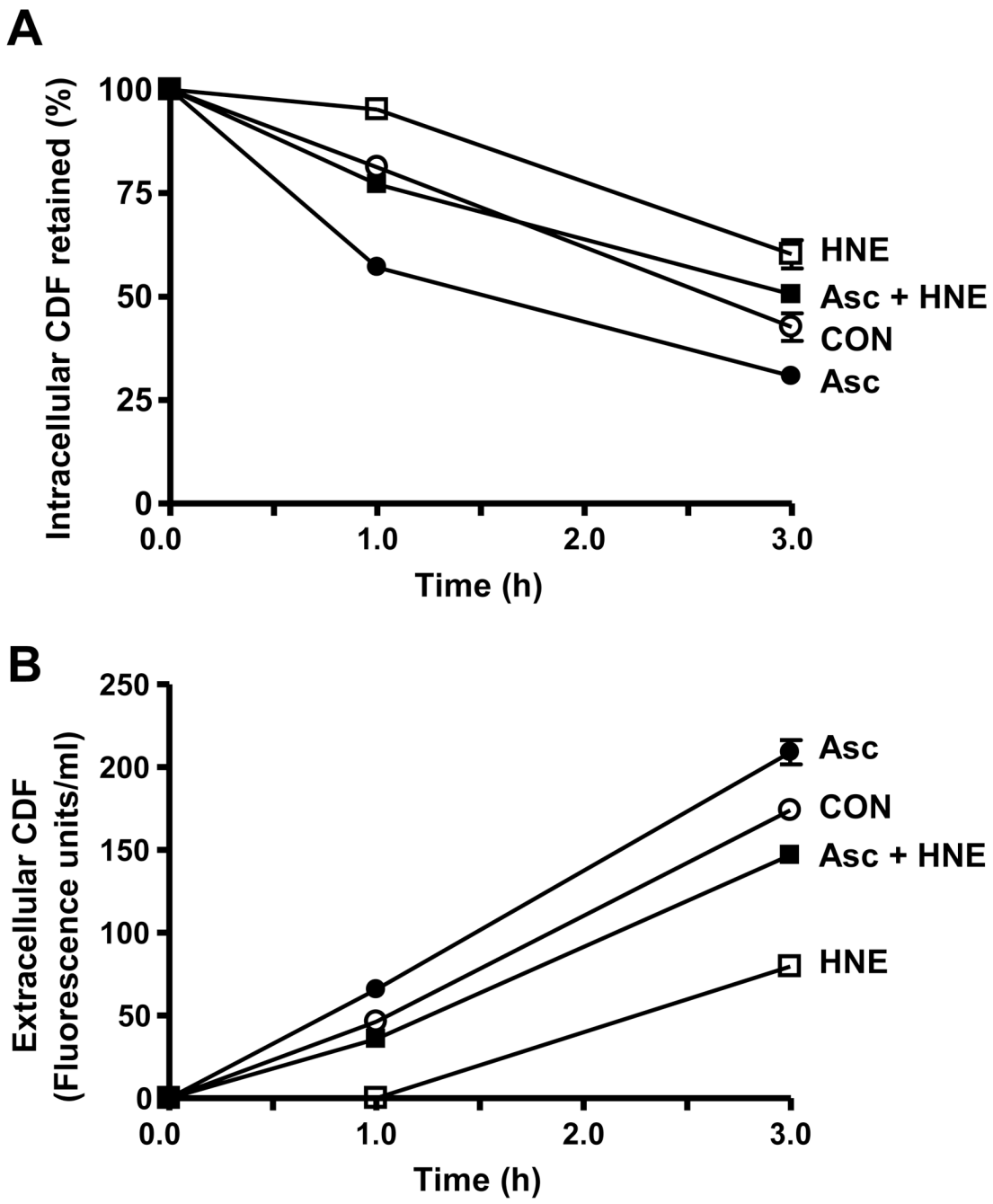

Figure 7.

Effect of Asc and HNE on the cellular retention (panel A) and release (panel B) of the MRP substrate, CDF, in THP-1 cells. The cells were incubated with Asc (1 mM) for 18 h, washed and reincubated for 3 h in HBSS with 3 μM CDFDA. After 30 min, the cells were washed and re-incubated in CDFDA-free HBSS containing 0.1 mM HNE for 1 or 3 h. Intracellular CDF and CDF released into the medium were then determined by spectrofluorometry. Values are expressed as means ± SE of 3 experiments. Data were analyzed by one-way analysis of variance (ANOVA) followed by the Tukey-Kramer multiple comparison post hoc test. All values are statistically different ($p \leq 0.05$) from each other at the 3 h time point.

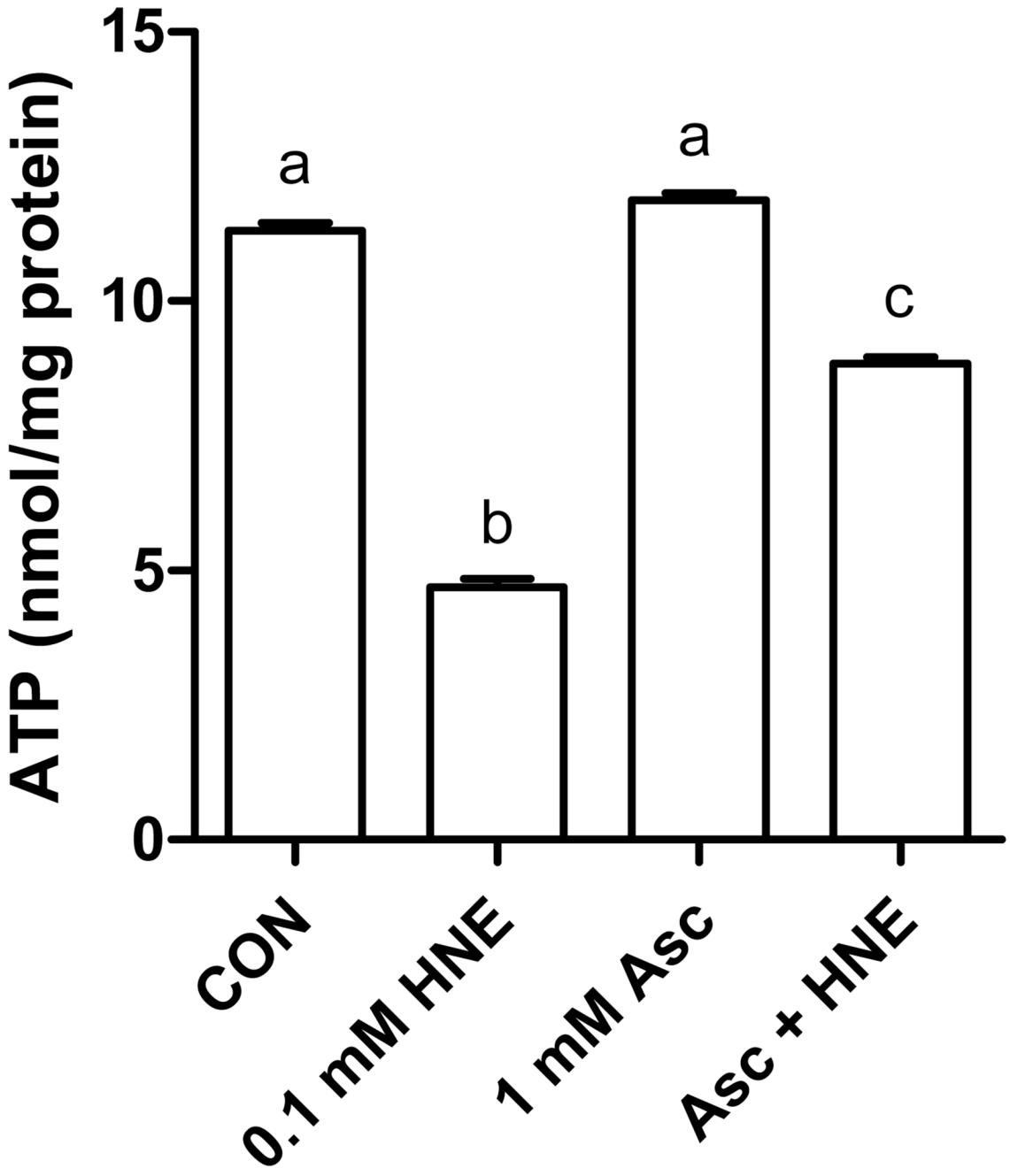

Figure 8.

Effect of Asc on HNE-induced depletion of ATP. Cells pre-incubated with 1 mM Asc for 18 h were washed with HBSS and incubated with 0.1 mM HNE in HBSS for 3 h before ATP analysis by HPLC. Values are expressed as means ± SE of 3 experiments. Data were analyzed by one-way analysis of variance (ANOVA) followed by the Tukey-Kramer multiple comparison post hoc test. All values are statistically different ($p \leq 0.05$) from each other except when sharing a common letter.

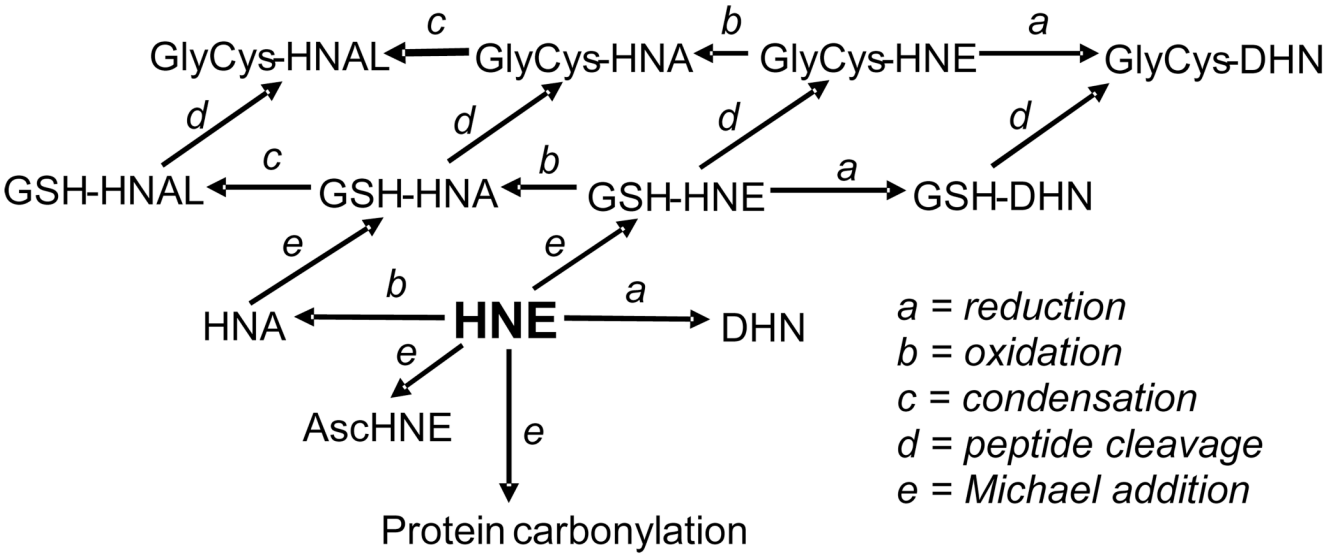

Scheme 1.
Fate of HNE in THP-1 monocytes.

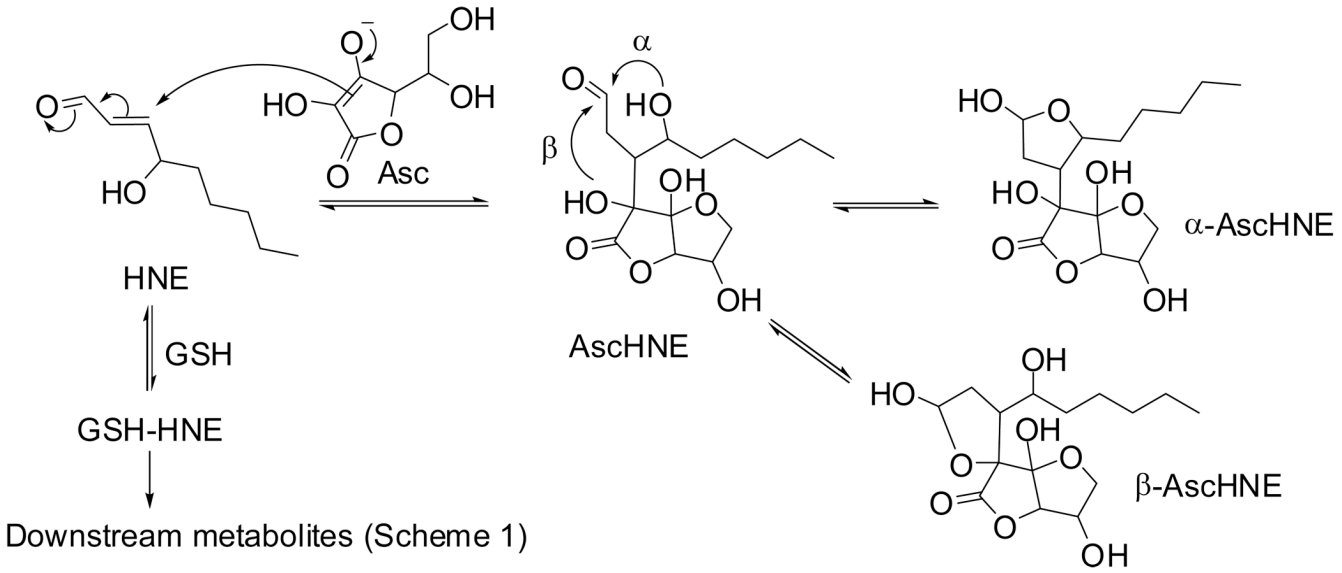

Scheme 2.
Ascorbylation of HNE.

Table 1

Effect of Asc on HNE metabolism and excretion in THP-1 cells

HNE metabolite	Effect of Asc on HNE conjugate formation expressed as the ratio of peak areas [a], $A_{Asc\text{-}adeq,\ avg}/A_{Asc\text{-}def,\ avg}$	*p*-value of effect of Asc [c]
GSH-HNAL	1.16	0.014
GSH-HNE	1.12	0.11
GSH-DHN	1.16	0.086
GlyCys-HNAL	1.11	0.33
GlyCys-HNE	1.11	0.20
GlyCys-DHN	1.06	0.61
	Effect of Asc on HNE conjugate distribution between medium and lysate expressed as the ratio [b], $R_{Asc\text{-}adeq,\ avg}/R_{Asc\text{-}def,\ avg}$	
GSH-HNAL	1.25	0.012
GSH-HNE	1.04	0.54
GSH-DHN	1.21	0.013
GlyCys-HNAL	0.95	0.40
GlyCys-HNE	1.16	0.048
GlyCys-DHN	1.16	0.040

[a] $A_{Asc\text{-}adeq}$ = Peak area recorded for metabolite *x* in medium + Peak area recorded for metabolite *x* in lysate of Asc-pretreated THP-1 cells. $A_{Asc\text{-}def}$ = Peak area recorded for metabolite *x* in medium + Peak area recorded for metabolite *x* in lysate of THP-1 cells that were not pre-treated with Asc. The average (avg) of three measurements was determined to calculate the ratio $A_{Asc\text{-}adeq,\ avg}/A_{Asc\text{-}def,\ avg}$ ($n = 3$). For instance, a ratio of 1.16 indicates a 16% increase of HNE conjugate formation resulting from Asc-pretreatment.

[b] $R_{Asc\text{-}adeq} = A_{Asc\text{-}adeq,\ medium}/A_{Asc\text{-}adeq,\ lysate}$ and $R_{Asc\text{-}def} = A_{Asc\text{-}def,\ medium}/A_{Asc\text{-}def,\ lysate}$. For instance, a ratio $R_{Asc\text{-}adeq,\ avg}/R_{Asc\text{-}def,\ avg}$ of 1.25 indicates a 25% increase of metabolite amount found in the medium relative to the lysate amount, resulting from Asc-pretreatment.

[c] The null hypothesis was $A_{Asc\text{-}adeq} = A_{Asc\text{-}def}$ or $R_{Asc\text{-}adeq} = R_{Asc\text{-}def}$ ($n = 3$).